Received: 11 May 2022 | Revised: 7 March 2023 | Accepted: 26 April 2023

DOI: 10.1002/rnc.6762

RESEARCH ARTICLE

WILEY

Event-triggered consensus Kalman filtering for time-varying networks and intermittent observations

Aviv Priel[1] | **Daniel Zelazo**[2]

[1]Department of Guidance, Navigation and Control, Lulav Space Ltd., Haifa, Israel

[2]Faculty of Aerospace Engineering, Technion - Israel Institute of Technology, Haifa, Israel

Correspondence
Daniel Zelazo, Faculty of Aerospace Engineering, Technion - Israel Institute of Technology, Haifa, Israel
Email: dzelazo@technion.ac.il

Funding information
Israel Science Foundation, Grant/Award Number: 2285/20

Abstract

This work introduces an improved design approach for distributed event-triggering consensus Kalman filtering (DETCKF). We consider a network of sensors that are able to observe a linear discrete-time stochastic process with known dynamics. The sensors cooperate through information exchange over a possibly time-varying communication network to obtain an estimate of the process state. We propose event-triggering conditions and consensus gains for which the error dynamics of the filter are stable. Both are derived from a Lyapunov-based stability analysis. We also propose an event-triggering scheme for scenarios in which some of the agents have intermittent observability of the process—that is, they are not able to measure the process dynamics. Under mild conditions on the sensing architecture, we show that even in this case it is possible to design a stable event-triggered estimate of the process state. We validate our results with numerical simulations and compare with other solutions in the literature.

KEYWORDS

distributed estimation, event-triggered estimation, multi-agent systems, sensor networks

1 | INTRODUCTION

Cooperative estimation refers to a group of agents, equipped with sensing devices and communicating capabilities, working together to achieve an improved estimate of some detectable process. This complex problem has been a major subject of interest in various research communities due to its wide range of applications including autonomous vehicles,[1,2] semiconductors,[3] Internet-of-Things,[4] mapping and localization,[5,6] and space research.[7] The recently enhanced wireless sensors manufacturing capabilities led to an increase in the scale (number of agents) for wireless sensor networks. Considering cooperative estimation, the latter have instigated the necessity to discuss constraints such as network bandwidth[8] and global plus local energy consumption.[9] Essentially, the trade-off between an estimator performance level and the data transmission required to obtain it came into mind. For some researchers,[10,11] the cost function is no longer solely based on estimation accuracy terms, but includes a penalty on the total energy consumption.

One of the mechanisms found in order to cope with these constraints is referred to as *distributed event-triggered estimation* (DETE).[12] In this scheme, each agent in the system retrieves or transmits information to its neighbors only

[Correction added on 8 June 2023, after first online publication: Daniel Zelazo's affiliation has been corrected in this version.]

when some rule is violated. The rule comprises a set of conditions which must be locally examined at each iteration step. Violation of the rule will trigger an event and information will be shared. Between events, the agents will run a Kalman based estimator that relies only on locally obtained information. The system aims to globally converge to the true process state.

In this work we consider the *consensus Kalman filter*, which was first introduced in References 13 and 14. This estimator employs a consensus algorithm term that is fused with a classical Kalman estimator structure. This provides, for a given communication topology, a mechanism which enables the utilization of neighboring information to improve the state estimate of each sensor node. In this estimator architecture, the measurement or the estimate of an agent is broadcast to it's neighboring agents at every time instance.

Traditionally, distributed state estimators such as the discrete consensus Kalman filter assume that measurements are acquired at every time step. This mechanism was outdated as constraints and restrictions on data transmission and bandwidth arose. In this direction, the consensus Kalman filter combined with an event-triggering mechanism is a subject of increasing interest in recent years. For example, in Reference 15, the *send on delta* (SoD) rule is discussed, where each agent transmits its local estimates to its neighbours only if the difference between the most recent transmitted estimate and the current estimate exceeds some threshold. The author of Reference 16 expanded this research while addressing data transmission from a sensor to its peer estimator, where the estimator-to-estimator communication is discussed. For this scenario, the event-trigger condition is based on measurements only. In Reference 17, the issue of intermittent observations was tackled by introducing a binary variable to the update equations.

It should be noted that, to our knowledge, no comparison has been made between this approach and the non-cooperative consensus Kalman filter (NCLKF), where each sensor implements a Kalman filter without any exchange of information from other sensors in the network. This comparison is insightful for the application designer in order to understand the benefits of implementing distributed approaches. Furthermore, many works dealing with this topic employ a consensus gain which is computed in a centralized manner and requires knowledge of global network properties.[15,18,19] This methodology is both difficult to implement and may require heavy computational power in case of large scale networks. More importantly, centralized methods are fragile and are not able to cope with time-varying communication architecture. In the survey paper,[20] recent works that employ a decentralized methodology to solve the cooperative estimation problem are presented. Specifically, the authors in References 21 and 22 constructed a decentralized mechanism to handle time-varying communication topologies assuming that the network varies with a binary distribution. However no solutions are available (to the authors knowledge) for a general time-varying networks scheme.

In this direction, our contributions are listed below:

(i) leveraging existing solutions from the literature, we propose an event-triggered consensus Kalman filter architecture. We provide both centralized and decentralized approaches for computing the consensus gain while ensuring the estimation error stability;
(ii) we propose an event-triggered consensus Kalman filter architecture for time-varying communication topologies. We also provide a strategy for scenarios where sensing agents may only be able to observe the process intermittently (i.e., due to occlusion between the sensor and process, malfunction, or other);
(iii) we provide extensive comparisons through numerical simulation between different schemes including the NCLKF where the energy consumption versus performance trade-off is discussed.

The article is organized as follows. Section 2 provides an overview of the event-triggered consensus Kalman filter estimator. In Section 3, we derive a consensus gain factor and event-triggering condition which ensures the asymptotic stability of the noiseless error dynamics. In addition, a decentralized consensus gain is proposed along with a suitable event-triggered condition. In section 4, scenarios with nonobservable agents are tackled. In Section 5 simulation results are presented and finally, concluding notes are made in Section 6.

Notations

Let $\mathbb{R}$ denote the set of real numbers, $\mathbb{R}^n$ the n-dimensional Euclidean space and $\mathbb{R}^{n\times m}$ the set of $n \times m$ real matrices. Let $\text{diag}\{M^i\}_{i=1}^n$ denote the block diagonal $nd \times nd$ matrix where the ith block is equal to $M^i \in \mathbb{R}^{d\times d}$, and let $[M]_{ij}$ denote the

ij-entry of the matrix M. The maximal and minimal eigenvalues of the matrix M are denoted by $\lambda_{\max}(M)$ and $\lambda_{min}(M)$, respectively. The notation $A \otimes B$ denotes the matrix Kronecker product of A and B.

2 | THE EVENT-TRIGGERED CONSENSUS KALMAN FILTER

In this section, we review the basic setup for constructing a distributed event-triggered consensus Kalman filter. We begin with reviewing existing consensus Kalman filter solutions and then present the transmission-based event-triggered mechanisms that will be incorporated into the consensus Kalman filter to form the ETCKF.

Consider a network comprising N interacting agents where the interaction topology can be described by an undirected graph $\mathcal{G} = (\mathcal{V}, \mathcal{E})$. Here, $\mathcal{V} = \{1, 2, \dots, N\}$ denotes the node set and $\mathcal{E} \subseteq \mathcal{V} \times \mathcal{V}$ denotes the edge set indicating which agents can exchange information with each other. In undirected graphs, information flow is always bi-directional, that is, $(u, v) \in \mathcal{E}$ implies $(v, u) \in \mathcal{E}$. We also consider directed graphs where information flow has a specific direction such that $(u, v) \in \mathcal{E}$ does not necessarily means that $(v, u) \in \mathcal{E}$. The neighborhood of a node $v \in \mathcal{V}$ is the set of agents incident to it, that is, $\mathcal{N}_v = \{u \in \mathcal{V} \mid (u, v) \in \mathcal{E}\}$. The graph can also be represented using the in-degree Laplacian matrix, $L \in \mathbb{R}^{N \times N}$, defined as $[L]_{ii} = |\mathcal{N}_i|$, and $[L]_{ij} = -1$ if $(j, i) \in \mathcal{E}$, and $[L]_{ij} = 0$ if $(j, i) \notin \mathcal{E}$.[23] Note that for undirected graphs, the (in-degree) Laplacian matrix is symmetric.

Each agent observes a linear discrete-time stochastic process described by the dynamics

$$\mathcal{P} : x_{k+1} = Ax_k + Bw_k, \tag{1}$$

where $x_k \in \mathbb{R}^n$ is the state vector and w_k is an additive white Gaussian noise such that $\mathbb{E}\left[w_k w_l^T\right] = Q\delta_{kl}$, where δ_{kl} is the Dirac Delta function. Each agent is capable of measuring the process state using the observation model

$$z_k^i = H^i x_k + v_k^i, \tag{2}$$

where $z_k^i \in \mathbb{R}^{m^i}$ is the measurement obtained by agent i, $H^i \in \mathbb{R}^{m^i \times n}$ is the observation matrix, and $v_k^i \in \mathbb{R}^{m^i}$ is a measurement noise assumed to also be additive white Gaussian noise with $\mathbb{E}\left[v_k^i (v_l^i)^T\right] = R^i \delta_{kl}$. Additionally we assume that $R^i \in \mathbb{R}^{m^i \times m^i}$ is invertible and that (A, H^i) make an observable pair for every agent.

The distributed consensus Kalman estimator (DCKE) was first proposed in Reference 24 and is constructed as

$$\hat{x}_k^i = \bar{x}_k^i + K_k^i \left(z_k^i - H^i \bar{x}_k\right) + C_k^i \sum_{j \in \mathcal{N}_i} \left(\bar{x}_k^j - \bar{x}_k^i\right), \tag{3}$$

where K^i and C^i are the Kalman and consensus gains of the ith agent, respectively, and $\hat{x}^i$ and $\bar{x}^i$ are the posteriori and a priori state estimate of the ith agent, respectively. The consensus Kalman estimator (3) is composed of a classic Kalman estimator term and a consensus term based on neighbors estimates.

In Reference 25, the optimal Kalman gain was derived by minimizing the local mean squared error (MSE) with respect to K_k^i. The optimal gain for each agent was found to be

$$K_k^i = C_k^i \sum_{j \in \mathcal{N}_i} \left(\bar{P}_k^{j,i} - \bar{P}_k^i\right) H^{iT} \left(R^i + H^i \bar{P}_k^i H^{iT}\right)^{-1} + \bar{P}_k^i H^{iT} \left(R^i + H^i \bar{P}_k^i H^{iT}\right)^{-1},$$

where $\bar{P}^i$ is the ith agent a priori error covariance and $\bar{P}^{j,i}$ is the ith and jth agents' a priori cross correlation term. The corresponding update equations incorporate two-hop neighbor information exchange. For example, in a complete graph this would mean that each agent would retrieve $N(N-1)$ cross correlation terms at each step. This served as the motivation to construct the following sub-optimal distributed consensus Kalman filter (SOCKF) which utilizes only (one hop) neighboring state estimates and discards the consensus terms from the error covariance and Kalman gain update

equations:[25]

$$\begin{cases} \textbf{Estimation} \\ K_k^i = \bar{P}_k^i H^{iT}\left(R^i + H^i \bar{P}_k^i H^{iT}\right)^{-1} \\ \hat{P}_k^i = F_k^i \bar{P}_k^i F_k^{iT} + K_k^i R^i K_k^{iT} \\ \hat{x}_k^i = \bar{x}_k^i + K_k^i\left(z_k^i - H^i \bar{x}_k\right) + C_k^i \sum\limits_{j\in\mathcal{N}_i}\left(\bar{x}_k^j - \bar{x}_k^i\right) \\ \textbf{Prediction} \\ \bar{x}_{k+1}^i = A\hat{x}_k^i \\ \bar{P}_{k+1}^i = A\hat{P}_k^i A^T + BQB^T \end{cases} \tag{4}$$

where $F_k^i = I - K_k^i H^i$. The omission of the consensus terms from the Kalman gain and error covariance update equation is justified with the assumption that the consensus gain is relatively small. We would like to emphasize that one must be careful while selecting a small consensus gain since this might lead the consensus component in the DCKE to be negligible, as shown in Reference 26. Nevertheless, in Reference 25 it was shown that (4) has stable estimator dynamics.

The distributed *event-triggered consensus Kalman estimator* (DETCKE) was first proposed by.[27] The DETCKE structure is given as

$$\hat{x}_k^i = \bar{x}_k^i + K_k^i\left(z_k^i - H^i \bar{x}_k^i\right) + C_k^i \sum_{j\in\mathcal{N}_i}\left(\tilde{x}_k^{ji} - \tilde{x}_k^{ii}\right). \tag{5}$$

Here, $\tilde{x}^{ji}$ denote the jth agent state propagation, used in the ith agent estimator, according to the following event triggering mechanism (ETM),

$$\tilde{x}_k^{ji} = \begin{cases} \bar{x}_k^j, & f_k^j\left(\{\tilde{x}_k^{sj}\}_{s\in\mathcal{N}_j\cup\{j\}}, \bar{x}_k^j\right) > 0 \\ A\tilde{x}_{k-1}^{ji}, & f_k^j\left(\{\tilde{x}_k^{sj}\}_{s\in\mathcal{N}_j\cup\{j\}}, \bar{x}_k^j\right) \le 0 \end{cases} \quad \forall\, j \in \mathcal{N}_i \cup \{i\}, \tag{6}$$

where $f_k^j\left(\{\tilde{x}_k^{sj}\}_{s\in\mathcal{N}_j\cup\{j\}}, \bar{x}_k^j\right)$ is the event triggering function comprising local network properties and locally computed estimates, evaluated by the jth agent in each step. Formally, if the event-triggered condition (ETC) $f_k^j\left(\{\tilde{x}_k^{sj}\}_{s\in\mathcal{N}_j\cup\{j\}}, \bar{x}_k^j\right) \le 0$ is satisfied, then the ith agent will continue propagating the most recent state prediction obtained from the jth agent (assuming they are neighbors). If the ETC is violated then the jth agent will broadcast its current state prediction as depicted in Figure 1. The function $f_k^j\left(\{\tilde{x}_k^{sj}\}_{s\in\mathcal{N}_j\cup\{j\}}, \bar{x}_k^j\right)$ holds a key role in the filter update equations. If not well formulated, this function could lead to the absence of events which may cause the local estimation errors to diverge. On the other hand, it may generate an event at each time instance such that the event-triggered consensus Kalman estimator, for all practical purposes, serves as the consensus Kalman estimator (3). We note that the authors in Reference 27 designed the ETF based on the Kullback–Leibler (KL) divergence.[28] In the following sections we shall utilize different approaches to construct the ETF.

3 | EVENT-TRIGGERED CONSENSUS KALMAN ESTIMATOR DESIGN

In this section we explore both centralized and decentralized approaches for designing the consensus gain term C_k^i in (5). Additionally, we explore an event-triggered mechanism to reduce transmission loads while ensuring the stability of estimators with form (5).

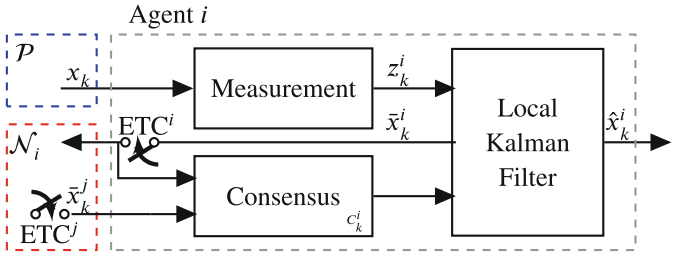

FIGURE 1 DETCKE structure for the ith agent where an agent transmits its state predictions once an event is triggered.

3.1 | Event-triggered condition for a centralized consensus gain

We now consider the consensus gain structure as proposed,

$$C_k^i = \gamma_k \hat{P}_k^i \left(F_k^i\right)^{-T}. \tag{7}$$

Additionally we consider the event-triggered condition for the ith agent, as proposed in Reference 18,

$$f_k^i\left(\{\tilde{x}_k^{ji}\}_{j\in\mathcal{N}_i\cup\{i\}}, \bar{x}_k^i\right) = \left(\bar{x}_k^i - \tilde{x}_k^{ii}\right)^T \sum_{j\in\mathcal{N}_i}\left(\tilde{x}_k^{ji} - \tilde{x}_k^{ii}\right) < 0. \tag{8}$$

Next we will propose a range of values for the consensus factor γ_k appearing in (7), that ensures the stability of the error dynamics of the estimator. This is presented in the following theorem.

Theorem 1 (DETCKE stability). *Consider a group of N agents interacting over an undirected, connected and static graph $\mathcal{G}$ with Laplacian matrix L, where each agent observes the process (1) with observation model (2). The noiseless estimation error for the DETCKE (5), the event-triggered mechanism (6) with the event-triggered condition (8), the choice of consensus gain $C_k^i = \gamma_k \hat{P}_k^i \left(F_k^i\right)^{-T}$ and any consensus factor satisfying*

$$0 \le \gamma_k \le \frac{2}{\lambda_{\max}\left(\operatorname{diag}\left\{\left(F_k^i\right)^{-1}\hat{P}_k^i\left(F_k^i\right)^{-T}\right\}_{i=1}^N\right)\lambda_{\max}(L)},$$

is asymptotically stable.

Proof. To prove the theorem, first we choose a quadratic Lyapunov function and show that for the suggested consensus factor and event-triggered condition, the Lyapunov function is monotonically decreasing. Let $\eta_k = \hat{x}_k - x_k$, $\bar{\eta}_k = \bar{x}_k - x_k$ and $\tilde{\eta}_k = \tilde{x}_k - x_k$ be the estimation, prediction, and propagation errors, respectively. The noiseless error dynamics are

$$\eta_k^i = \underbrace{(I - K_k^i H^i)}_{F_k^i}\bar{\eta}_k^i + C_k^i \sum_{j\in\mathcal{N}_i}\left(\tilde{\eta}_k^{ji} - \tilde{\eta}_k^{ii}\right)$$
$$\bar{\eta}_{k+1}^i = A\eta_k^i.$$

For notational convenience, we define

$$\tilde{u}_k^i = \sum_{j\in\mathcal{N}_i}\left(\tilde{\eta}_k^{ji} - \tilde{\eta}_k^{ii}\right),$$

representing the consensus term in the dynamics. Consider now the following Lyapunov function,

$$V_k = \sum_{i=1}^N (\eta_k^i)^T (\hat{P}_k^i)^{-1}\eta_k^i. \tag{9}$$

We define the Lyapunov step difference function $\delta V_k = V_k - V_{k-1}$. The Lyapunov difference along the system trajectories is

$$\begin{aligned}\delta V_k &= \sum_{i=1}^{N}(\eta_k^i)^T(\hat{P}_k^i)^{-1}\eta_k^i - \sum_{i=1}^{N}(\eta_{k-1}^i)^T(\hat{P}_{k-1}^i)^{-1}\eta_{k-1}^i \\ &= \sum_{i=1}^{N}\left(F_k^iA\eta_{k-1}^i + C_k^i\tilde{u}_k^i\right)^T(\hat{P}_k^i)^{-1}\left(F_k^iA\eta_{k-1}^i + C_k^i\tilde{u}_k^i\right) - (\eta_{k-1}^i)^T(\hat{P}_{k-1}^i)^{-1}\eta_{k-1}^i \\ &= \sum_{i=1}^{N}(\eta_{k-1}^i)^T\left(A^T(F_k^i)^T(\hat{P}_k^i)^{-1}F_k^iA - (\hat{P}_{k-1}^i)^{-1}\right)\eta_{k-1}^i + 2\sum_{i=1}^{N}(\bar{\eta}_k^i)^T(F_k^i)^T(\hat{P}_k^i)^{-1}C_k^i\tilde{u}_k^i + \sum_{i=1}^{N}(\tilde{u}_k^i)^T(C_k^i)^T(\hat{P}_k^i)^{-1}C_k^i\tilde{u}_k^i.\end{aligned}$$

It was shown in Reference 26 that the matrix $\Psi_k^i = A^T(F_k^i)^T(\hat{P}_k^i)^{-1}F_k^iA - (\hat{P}_{k-1}^i)^{-1}$ satisfies $\Psi_k^i < 0$, that is, it is negative definite. Recall the consensus gain structure from (7),

$$C_k^i = \gamma_k\hat{P}_k^i(F_k^i)^{-T} = \gamma_k\bar{P}_k^i, \tag{10}$$

where the second equality stems from the well-known result in Kalman filtering that $\hat{P}_k = F_k\bar{P}_k$ (see Reference 29). Inserting (10) into δV_k produces

$$\delta V_k = \sum_{i=1}^{N}(\eta_{k-1}^i)^T\Psi_k^i\eta_{k-1}^i + 2\gamma_k\sum_{i=1}^{N}(\bar{\eta}_k^i)^T\tilde{u}_k^i + \gamma_k^2\sum_{i=1}^{N}(\tilde{u}_k^i)^TY_k^i\tilde{u}_k^i, \tag{11}$$

where $Y_k^i = \left(F_k^i\right)^{-1}\hat{P}_k^i\left(F_k^i\right)^{-T}$.

We now consider the event-trigger condition for the ith agent,

$$\begin{aligned}f_k^i\left(\{\tilde{x}_k^{ji}\}_{j\in\mathcal{N}_i\cup\{i\}}, \bar{x}_k^i\right) &= \left(\bar{x}_k^i - \tilde{x}_k^{ii}\right)^T\tilde{u}_k^i \\ &= \left(\bar{\eta}_k^i - \tilde{\eta}_k^{ii}\right)^T\tilde{u}_k^i \le 0.\end{aligned} \tag{12}$$

If ETC (12) is violated, then according to ETM (6) we obtain that $\bar{x}_k^i = \tilde{x}_k^{ii}$ or equivalently $\bar{\eta}_k^i = \tilde{\eta}_k^{ii}$ such that:

$$2\gamma_k(\bar{\eta}_k^i)^T\tilde{u}_k^i = 2\gamma_k(\tilde{\eta}_k^{ii})^T\tilde{u}_k^i.$$

If ETC (12) is satisfied, then the following inequality holds:

$$2\gamma_k(\bar{\eta}_k^i)^T\tilde{u}_k^i \le 2\gamma_k(\tilde{\eta}_k^{ii})^T\tilde{u}_k^i. \tag{13}$$

Thus the second term in (11) satisfies

$$2\gamma_k\sum_{i=1}^{N}(\bar{\eta}_k^i)^T\tilde{u}_k^i \le 2\gamma_k\sum_{i=1}^{N}(\tilde{\eta}_k^{ii})^T\tilde{u}_k^i, \tag{14}$$

for each time step k. Additionally, we know that $\tilde{x}^{ji}$ is the same for all $i \in \mathcal{N}_j$, that is,

$$\tilde{x}^{ji} = \tilde{x}^{js}\ \forall\ \{i,s\} \in \mathcal{N}_j,$$

such that the following equality holds,

$$\tilde{u}_k = (L \otimes I_n)\,\tilde{\eta}, \tag{15}$$

with $\tilde{u}_k = \left[(\tilde{u}_k^1)^T\ (\tilde{u}_k^2)^T\ \cdots\ (\tilde{u}_k^N)^T\right]^T$. Fusing (14) and (15) into (11) yields

$$\begin{aligned}\delta V_k &= \sum_{i=1}^{N}(\eta_{k-1}^i)^T\Psi_k^i\eta_{k-1}^i + 2\gamma_k\sum_{i=1}^{N}(\bar{\eta}_k^i)^T\tilde{u}_k^i + \gamma_k^2\sum_{i=1}^{N}(\tilde{u}_k^i)^T Y_k^i\tilde{u}_k^i\\ &< 2\gamma_k\sum_{i=1}^{N}(\tilde{\eta}_k^{ii})^T\tilde{u}_k^i + \gamma_k^2\lambda_{\max}(Y_k)\sum_{i=1}^{N}(\tilde{u}_k^i)^T\tilde{u}_k^i\\ &\le -2\gamma_k\tilde{\eta}_k^T(L\otimes I_n)\tilde{\eta}_k + \gamma_k^2\lambda_{\max}(Y_k)\tilde{\eta}_k^T(L\otimes I_n)(L\otimes I_n)\tilde{\eta}_k\\ &\le -(2\gamma_k - \gamma_k^2\lambda_{\max}(Y_k)\lambda_{\max}(L))\tilde{\eta}_k^T(L\otimes I_n)\tilde{\eta}_k \le 0,\end{aligned} \tag{16}$$

where $Y_k = \text{diag}\{Y_k^i\}_{i=1}^N$. Hence, for any consensus factor which satisfies

$$0 \le \gamma_k \le \frac{2}{\lambda_{\max}(Y_k)\lambda_{\max}(L)}, \tag{17}$$

the Lyapunov difference (11) is strictly decreasing. ∎

It should be noted that by choosing $\gamma_k = 0$, we obtain the NCLKF for which stability is ensured. We have shown that by selecting a consensus factor which satisfies (17), consensus gain structure (7), and ETC (12), we are able to guarantee the stability of the noiseless estimation error. Note that the upper-bound for γ_k in (17) is a function of a global property of the network, $\lambda_{\max}(L)$, leading to a centralized computation, as illustrated in Figure 2. From a practical standpoint this bound can only be useful if the underlying communication graph is static. However, in most-real world scenarios, this assumption cannot be assumed. This motivates the next section of this work, where we propose a consensus gain that can be computed both distributedly and as a function of only local neighborhood properties, thus ensuring robustness against time-varying communication topologies.

Remark 1. The consensus gain proposed in Reference 18 has the form

$$C_k^i = \frac{2F_k^i\Gamma_k^{i-1}}{\lambda_{\max}(\Gamma_k^{-1})\,\lambda_{\max}(L)}, \tag{18}$$

where $\Gamma_k^i = \left(F_k^i\right)^T A^T(\bar{P}_k^i)^{-1}AF_k^i$ and $\Gamma_k = \text{diag}\{\Gamma_k^i\}_{i=1}^N$. The computation of (18) requires the assumption that the matrix A is nonsingular. However, even if it is nonsingular but ill-conditioned, it may still lead to numerical challenges. This is in contrast to the gain proposed in this work that does not require inversion of the process dynamics. The performance degradation of (18) with respect to the consensus gain stated in Theorem 1 will be presented in Section 5.

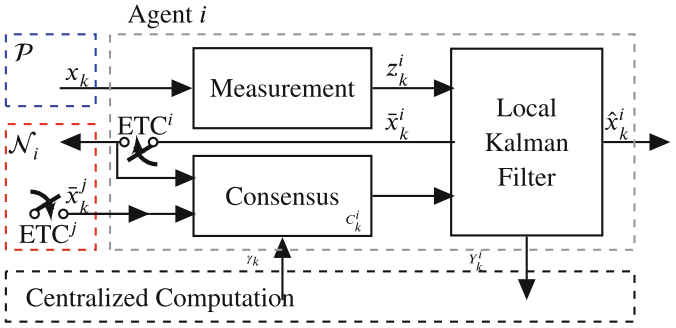

FIGURE 2 DETCKE structure for the ith agent–centralized consensus gain architecture.

3.2 | Event-triggered condition for a decentralized consensus gain

In the previous subsection we proposed a centralized solution for the determination of the consensus factor γ_k that required global network information, that is, the largest eigenvalue of the Laplacian matrix L and the augmented matrix Y_k. In our previous work,[26] we showed that this choice of gain can be problematic for time-varying communication networks. Additionally, for large-scale networks, the centralized architecture may also require heavy computational tools. In this subsection, we propose a decentralized event-trigger scheme in which the event-triggering function and the consensus factor are formulated such that only local network properties are required.

Consider a group of N agents, interacting over a time-varying and undirected communication graph, denoted by $\mathcal{G}_k$. Each sensor observes the process (1) with observation model (2) and the consensus Kalman estimator:

$$\hat{x}_k^i = \bar{x}_k^i + K_k^i\left(z_k^i - H^i\bar{x}_k^i\right) + C_k^i\sum_{j\in\mathcal{N}_{i,k}}\beta_k^j\left(\bar{x}_k^j - \bar{x}_k^i\right), \tag{19}$$

where $\mathcal{N}_{i,k}$ is neighborhood of the ith agent with respect to the graph $\mathcal{G}_k$, $\beta_k^j = 1$ if the jth agent broadcasts its information and $\beta_k^j = 0$, otherwise. In (19), we use the broadcasting neighbors a priori state prediction in the consensus term instead of the state propagation $\tilde{x}_k^{ji}$ of nonbroadcasting agents as formulated in (5). In this direction, we introduce the following ETM:

$$\beta_k^j = \begin{cases} 1, & f_k^j\left(\{\tilde{x}_k^{sj}\}_{s\in\mathcal{N}_j\cup\{j\}}, \bar{x}_k^j\right) > 0 \\ 0, & f_k^j\left(\{\tilde{x}_k^{sj}\}_{s\in\mathcal{N}_j\cup\{j\}}, \bar{x}_k^j\right) \le 0 \end{cases} \quad \forall\, j\in\mathcal{N}_i\cup\{i\}. \tag{20}$$

Additionally, we consider the SoD event-triggering condition for the jth agent:

$$f_k^j\left(\{\tilde{x}_k^{sj}\}_{s\in\mathcal{N}_j\cup\{j\}}, \bar{x}_k^j\right) = \|\tilde{x}_k^{jj} - \bar{x}_k^j\|^2 - \delta \le 0, \tag{21}$$

where $\tilde{x}^{ij}$ is formulated as in (6) and $\delta\in\mathbb{R}$ is some constant threshold so that an agent will broadcast (trigger an event) if the error norm between the state prediction and the state propagation exceeds some value.

To simplify future discussion, we introduce a new notation set to describe the instantaneous broadcast channels of an event-triggering scheme. Let L_k be the Laplacian matrix for the sensing network $\mathcal{G}_k$ describing the available communication channels between each agent at step k. Let $\mathcal{G}_k^* = \left(\mathcal{V}, \mathcal{E}_k^*\right)$ denote the transmission graph of agents for which an event was triggered such that

$$\mathcal{E}_k^* = \{(j,i) \mid \beta_k^j = 1, j\in\mathcal{N}_{i,k}\}.$$

Additionally, let L_k^* be the Laplacian matrix for the directed sensing network $\mathcal{G}_k^*$. Finally, let $\mathcal{N}_{i,k}^*$ be the local neighborhood of the ith agent with respect to $\mathcal{G}_k^*$ such that $\mathcal{N}_{i,k}^* = \{j \mid \beta_k^j = 1, i\in\mathcal{N}_{j,k}\}$.

Thus, (19) can be reformulated as

$$\hat{x}_k^i = \bar{x}_k^i + K_k^i\left(z_k^i - H^i\bar{x}_k^i\right) + C_k^i\sum_{j\in\mathcal{N}_{i,k}^*}\left(\bar{x}_k^j - \bar{x}_k^i\right). \tag{22}$$

We now consider the following consensus gain,

$$C_k^i = \begin{cases} \frac{1}{|\mathcal{N}_{i,k}^*|+1}F_k^i, & |\mathcal{N}_{i,k}^*| > 0 \\ 0, & |\mathcal{N}_{i,k}^*| = 0 \end{cases}. \tag{23}$$

Note that for the case where an agent has no broadcasting neighbors, that is, $|\mathcal{N}^*_{i,k}| = 0$, the consensus term will be zero and the agent will run the NCLKF. In this case it is straightforward that the noiseless error dynamics are

$$\begin{aligned} \eta^i_k &= F^i_k \bar{\eta}^i_k \\ \bar{\eta}^i_{k+1} &= A\eta^i_k. \end{aligned} \tag{24}$$

For the nonempty neighborhood case, the local noiseless error dynamics are

$$\begin{aligned} \eta^i_k &= F^i_k \bar{\eta}^i_k + \frac{1}{|\mathcal{N}^*_{i,k}|+1} F^i_k \sum_{j\in\mathcal{N}^*_{i,k}} \left(\bar{\eta}^j_k - \bar{\eta}^i_k\right) \\ &= F^i_k \bar{\eta}^i_k + \left(\frac{1}{|\mathcal{N}^*_{i,k}|+1} F^i_k \sum_{j\in\mathcal{N}^*_{i,k}} \bar{\eta}^j_k\right) - \frac{|\mathcal{N}^*_{i,k}|}{|\mathcal{N}^*_{i,k}|+1} F^i_k \bar{\eta}^i_k \\ &= \frac{1}{|\mathcal{N}^*_{i,k}|+1} F^i_k \sum_{j\in\mathcal{N}^*_{i,k}\cup\{i\}} \bar{\eta}^j_k \\ \bar{\eta}^i_{k+1} &= A\eta^i_k, \end{aligned} \tag{25}$$

and the augmented noiseless error dynamics are

$$\begin{aligned} \eta_k &= \operatorname{diag}\{F^i_k A\}^N_{i=1} \left(I_{Nn} - \left(\mathcal{D}^{-1}_k L^*_k \otimes I_n\right)\right) \eta_{k-1} \\ &= \operatorname{diag}\{F^i_k\}^N_{i=1} ((I_N - \mathcal{D}^{-1}_k L^*_k) \otimes A)\eta_{k-1}, \end{aligned} \tag{26}$$

with $\mathcal{D}_k = \operatorname{diag}\{|\mathcal{N}^*_{i,k}|+1\}^N_{i=1}$.

Under the case where each sensor has the same observation of the process, we can arrive at the following result.

Theorem 2. *Assume that each sensor in the network measures the process (1) using the same observation model*

$$z^i_k = Hx_k + v^i_k, \quad i = 1, \dots, N,$$

where v^i_k is the zero-mean Gaussian measurement noise with $\mathbb{E}[v^i_k (v^i_l)^T] = R\delta_{kl}$. Additionally, assume that each agent activates the event-triggered consensus Kalman filter (22) with the consensus gain (23) and the event-triggered mechanism with event trigger condition (21) over a time-varying communication graph $\mathcal{G}_k$. Then the error dynamics (26) are asymptotically stable.

Proof. In the case where each sensor uses the same measurement model, it follows that $F^i_k = \bar{F}_k$ for all agents. The error dynamics can then be simplified to

$$\begin{aligned} \eta_k &= \operatorname{diag}\{F^i_k A\}^N_{i=1} \left(I_{Nn} - \left(\mathcal{D}^{-1}_k L^*_k \otimes I_n\right)\right) \eta_{k-1} \\ &= (I_N \otimes \bar{F}_k A)((I_N - \left(\mathcal{D}^{-1}_k L^*_k\right)) \otimes I_n) \eta_{k-1} \\ &= \left((I_N - (\mathcal{D}^{-1}_k L^*_k)) \otimes \bar{F}_k A\right) \eta_{k-1}. \end{aligned}$$

Due to the properties of the Kronecker product, we have that $(I_N \otimes \bar{F}_k A)$ and $((I_N - (\mathcal{D}^{-1}_k L^*_k)) \otimes I_n)$ commute. This leads to the following inequality,

$$\lim_{k\to\infty} \left\| \prod_k \left((I_N - (\mathcal{D}^{-1}_k L^*_k)) \otimes \bar{F}_k A\right) \right\| \le \lim_{k\to\infty} \left\| \prod_k (\bar{F}_k A) \right\| \lim_{k\to\infty} \left\| \prod_k (I_N - (\mathcal{D}^{-1}_k L^*_k)) \right\|.$$

From the stability of the NCLKF, it follows that $\lim_{k\to\infty} \left(\prod_k \bar{F}_k A\right) = 0$. If ETC (21) is satisfied for all agents events we have that $\left(I_N - \mathcal{D}^{-1}_k L^*_k\right) = I_N$, while if ETC (21) is violated for some agents, the Laplacian L^*_k will correspond to the new instantaneous topology and will not necessarily be symmetric. Finally, if ETC (21) is violated for all agents then $L^*_k = L_k$. For all mentioned scenarios, the matrix $\left(I_N - \mathcal{D}^{-1}_k L^*_k\right)$ is row stochastic at each time

step k, and thus its spectral radius is always unity, and in particular,

$$\rho\left(\lim_{k\to\infty}\left(\prod_k (I_N - \mathcal{D}_k^{-1}L_k^*)\right)\right) = 1,$$

since the product of row-stochastic matrices are row-stochastic. Therefore,

$$\lim_{k\to\infty}\eta_k = \lim_{k\to\infty}\left(\prod_k \left(I_N - (\mathcal{D}_k^{-1}L_k^*)\right)\otimes\prod_k \bar{F}_k A\right)\eta_0 = 0,$$

and the noiseless error dynamics are asymptotically stable. ∎

The result of Theorem 2 is restricted to the homogeneous case where each sensor has the same measurement noise characteristics. Although the proof for the stability of the heterogeneous case is not given in this article, we note that numerical simulations show promising results; we explore this in Section 5.

So far we have discussed cases where the process is observable by each node in the sensors network. We now wish to expand our results by constructing a strategy to cope with real-life scenarios such as sensors that may only function intermittently, for example due to occlusion between the sensor and the process, or malfunction. This issue is tackled in the following section.

4 | EVENT-TRIGGERED CONSENSUS KALMAN ESTIMATORS WITH INTERMITTENT OBSERVABILITY

In this section we shall relax the assumption where all agents are able to measure the process (1). We consider the scenario where the sensing agents have a fixed sensing radius r, and a measurement is available only when the process state is within this radius. Formally, let $p^i \in \mathbb{R}^d$ be the fixed position of sensor i for $d \in \{2, 3\}$. Then the measurement model for each sensing agent now has the form

$$z_k^i = \begin{cases} Hx_k + v_k^i, & \|h(x_k) - p^i\| \le r \\ \emptyset, & \text{otherwise} \end{cases}, \tag{27}$$

where $z_k^i = \emptyset$ means that there is no measurement available to agent i. Since the process state x_k may not represent its physical position in $\mathbb{R}^d$, we introduce the map $h : \mathbb{R}^n \to \mathbb{R}^d$ that maps its state to its position. This measurement model is illustrated in Figure 3A. Here, the process state is indicated by the black node. All the blue nodes are able to sense the process, while the red nodes are not. At the same time, the sensor agents are able to exchange information with each other according to the underlying communication graph, indicated by edges in the figure. Note that as the process state moves, the sensing agents may also change.

To cope with this scenario, we introduce some new notations to capture the state-dependent nature of the sensing network. First, we consider the network $\mathcal{G} = (\mathcal{V}, \mathcal{E})$ of N sensing agents with an undirected communication topology (see Figure 3A). Let L be the Laplacian matrix for the sensing network $\mathcal{G}$ describing the available communication channels between each agent. Let $\mathcal{O}_k \subseteq \mathcal{V}$ denote the set of agents that are able to measure the process according to (27) at time-step k, and let $\bar{\mathcal{O}}_k$ be the set of agents that are not able to measure the process. Thus it holds that $\mathcal{O}_k \cup \bar{\mathcal{O}}_k = \mathcal{V}$ for all k. We define a directed network architecture to reflect the difference between the sensing and nonsensing nodes. This leads to a time varying and directed communication graph (see Figure 3B) which is denoted by $\hat{\mathcal{G}}_k$. The edge set of $\hat{\mathcal{G}}_k$ is thus determined by which agents can observe the process. Nonobserving nodes do not share any information with other nodes, but are able to receive information from the sensing nodes. Let

$$\begin{aligned} \mathcal{E}_{\mathcal{O}_k,\bar{\mathcal{O}}_k} &= \{(i,j) \mid i \in \mathcal{O}_k,\ j \in \bar{\mathcal{O}}_k, \{i,j\} \in \mathcal{E}\}, \\ \mathcal{E}_{\mathcal{O}_k,\mathcal{O}_k} &= \{(i,j) \mid i,j \in \mathcal{O}_k, \{i,j\} \in \mathcal{E}\}, \end{aligned} \tag{28}$$

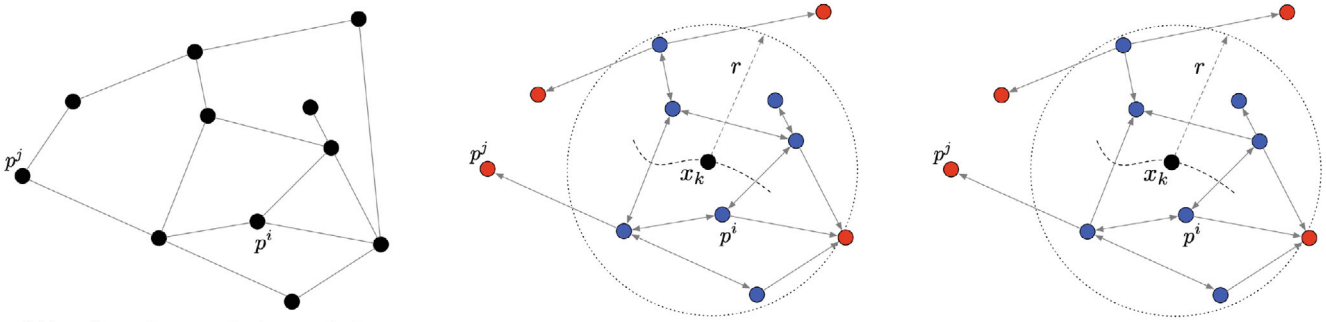

(A) Undirected communication graph $\mathcal{G}$. (B) Directed state-dependent graph $\hat{\mathcal{G}}_k$. (C) Broadcast graph $\mathcal{G}_k^\star$.

FIGURE 3 Example of (A) the communication graph $\mathcal{G}$. The edges indicate which agents may be able to communicate with each other. However, only agents inside the disc around the process obtain an observation (the blue nodes), leading to the directed graph $\hat{\mathcal{G}}_k$ in (B). The graph in (C) indicates a possible broadcast graph determined by the ETC. Notice that not all sensing nodes need broadcast. However, any sensing node connected to a nonsensing node (red nodes) must broadcast.

be the set of edges connecting the observing agents to the nonobserving agents, and observing agents with observing agents, respectively. Thus, $\hat{\mathcal{G}}_k = (\mathcal{V}, \mathcal{E}_{\mathcal{O}_k,\mathcal{O}_k} \cup \mathcal{E}_{\mathcal{O}_k,\bar{\mathcal{O}}_k}) = (\mathcal{V}, \hat{\mathcal{E}}_k)$. Note that the observing agents have bidirectional edges between them, while nonobserving agents only have incoming edges emanating from the observing agents. This is illustrated in Figure 3B.

We make the following assumption on the time-varying structure of the graph $\hat{\mathcal{G}}_k$.

Assumption 1. The graph $\hat{\mathcal{G}}_k$ is weakly connected at each time k. Equivalently, there exists a directed path from every observing agent in $\mathcal{O}_k$ to every nonobserving agent in $\bar{\mathcal{O}}_k$, and $|\mathcal{O}_k| \geq 1$.

We now wish to extend our discussion by accounting for energy consumption in the form of communication loads. This shall be done for observing agents only, as nonobserving agents shall not broadcast information according to the aforementioned architecture. This distinction is made clear using the following ETM,

$$\beta_k^j = \begin{cases} 1, & f_k^j\left(\{\tilde{x}_k^{sj}\}_{s\in\mathcal{N}_j\cup\{j\}}, \bar{x}_k^j\right) > 0 \\ 0, & f_k^j\left(\{\tilde{x}_k^{sj}\}_{s\in\mathcal{N}_j\cup\{j\}}, \bar{x}_k^j\right) \leq 0 \end{cases}, \tag{29}$$

where $\beta_k^j = 1$ means that the jth agent is broadcasting its state information and $\beta_k^j = 0$ means it does not broadcast. Additionally, the following ETF is used,

$$f_k^j\left(\{\tilde{x}_k^{sj}\}_{s\in\mathcal{N}_j\cup\{j\}}, \bar{x}_k^j\right) = \begin{cases} -1, & j \in \bar{\mathcal{O}}_k \\ 1, & j \in \cup_{i\in\bar{\mathcal{O}}_k}\mathcal{N}_i\ ,\ j \in \mathcal{O}_k \\ \left(\bar{x}_k^j - \tilde{x}_k^{jj}\right)^T\left(\bar{x}_k^j - \tilde{x}_k^{jj}\right) - \delta, & j \notin \cup_{i\in\bar{\mathcal{O}}_k}\mathcal{N}_i\ ,\ j \in \mathcal{O}_k \end{cases}, \tag{30}$$

where $\tilde{x}^{jj}$ is formulated as in (6), $\delta \in \mathbb{R}$ is some constant threshold, and $\mathcal{N}_i$ denote the neighborhood of the ith agent with respect to the sensing graph $\mathcal{G}$. The event-triggering function (30) is constructed such that nonobserving agent will not broadcast their state estimation so that $\beta_k^j = 0 \forall j \in \bar{\mathcal{O}}_k$. Furthermore, observing agents which are neighbors to nonobserving agents will constantly broadcast their state estimation so that $\beta_k^j = 1\ \forall j \in \mathcal{O}_k \cap \left(\cup_{i\in\bar{\mathcal{O}}_k}\mathcal{N}_i\right)$. This ensures Assumption 1 holds. Finally, observing agents with no nonobserving neighbors will broadcast their estimates based on the SoD event trigger condition so that β_k^j value is modified accordingly.

Let $\mathcal{G}_k^* = \left(\mathcal{V}, \mathcal{E}_k^*\right)$ denote the transmission graph of broadcasting agents at step k. The edge set of $\mathcal{G}_k^*$ is thus determined by which agents are broadcasting such that $\mathcal{E}_k^* = \{(j,i) \mid \beta_k^j = 1, j \in \mathcal{N}_i\}$. Additionally, let L_k^* be the Laplacian matrix for the directed sensing network $\mathcal{G}_k^*$.

To summarize, we have introduced three communication graphs: the available undirected communication graph $\mathcal{G}$ (Figure 3A), the weakly connected communication graph $\hat{\mathcal{G}}_k$ introduced to cope with partial nonobservability (Figure 3B), and the graph $\mathcal{G}_k^*$ introduced to describe the instantaneous broadcasting nature of an event-triggered scheme (Figure 3C). Note that $\mathcal{E}_k^* \subseteq \hat{\mathcal{E}}_k$.

We note that for this configuration, in order to ensure stability of the error dynamics, the consensus factor must be reevaluated. This is due to the fact that the noiseless error dynamic for agents with no observations of the process are not necessarily asymptotically stable in the noncooperative case. In fact, since in this scenario a nonobserving agent is just propagating the state, we would expect to see the error diverge in some cases. Thus, the proof that was given in Section 3.1 is incompatible.

Additionally, the state estimator must be reconstructed as well. In this direction we consider the following event-triggered consensus Kalman estimator:

$$\hat{x}_k^i = \begin{cases} \bar{x}_k^i + K_k^i(z_k^i - H_k\bar{x}_k^i) + C_k^i u_k^i, & i \in \mathcal{O}_k \\ \bar{x}_k^i + C_k^i u_k^i, & i \in \bar{\mathcal{O}}_k \end{cases}, \tag{31}$$

where

$$u_k^i = \sum_{j\in\mathcal{N}_i} \beta_k^j \left(F_k^j \bar{x}_k^j - F_k^i \bar{x}_k^i\right),$$

and $F_k^i = I - K_k^i H$. Note that the innovation term nullifies for the nonobserving case as no local measurements are obtained.

Now that our setup is complete, we may proceed to the stability analysis for the described configuration. Under the case where each observing agent has the same observation of the process, we can arrive at the following result.

Theorem 3 (stability with partial observability). *Consider a group of N agents interacting over a time-varying graph $\hat{\mathcal{G}}_k = (\mathcal{V}, \mathcal{E}_{\mathcal{O}_k,\mathcal{O}_k} \cup \mathcal{E}_{\bar{\mathcal{O}}_k,\mathcal{O}_k})$ as defined in (28) and satisfying Assumption 1, where each agent observes the process (1) with the same state-dependent observation model (27). Let the event-triggered consensus Kalman estimator be of type (31). Additionally, let the event-triggered mechanism be given as (29) with the event-triggered condition (30). Finally, let the consensus gain be given as*

$$C_k^i = \begin{cases} \dfrac{1}{1+\sum_{j\in\mathcal{N}_i}\beta_k^j} & i \in \mathcal{O}_k \\ \dfrac{1}{\sum_{j\in\mathcal{N}_i}\beta_k^j} & i \in \bar{\mathcal{O}}_k \end{cases}. \tag{32}$$

Then the noiseless estimation error is asymptotically stable.

Proof. We begin our proof by constructing the error dynamics for the observing agents and nonobserving agents. Next we construct the joint error dynamics and prove that it is asymptotically stable.

In the case where each observing sensor uses the same measurement model, it follows that $F_k^i = \bar{F}_k \forall i \in \mathcal{O}_k$. Thus, the error dynamics for observing agents are:

$$\begin{aligned} \eta_k^i &= \bar{F}_k\bar{\eta}_k^i + \frac{1}{1+\sum_{j\in\mathcal{N}_i}\beta_k^j}\bar{F}_k\sum_{j\in\mathcal{N}_i}\beta_k^j\left(\bar{\eta}_k^j - \bar{\eta}_k^i\right) \\ &= \bar{F}_k\bar{\eta}_k^i + \left(\frac{1}{1+\sum_{j\in\mathcal{N}_i}\beta_k^j}\bar{F}_k\sum_{j\in\mathcal{N}_i}\beta_k^j\bar{\eta}_k^j\right) - \frac{\sum_{j\in\mathcal{N}_i}\beta_k^j}{1+\sum_{j\in\mathcal{N}_i}\beta_k^j}\bar{F}_k\bar{\eta}_k^i \end{aligned}$$

$$= \frac{1}{1+\sum_{j\in\mathcal{N}_i}\beta_k^j}\bar{F}_k\left(\bar{\eta}_k^i + \sum_{j\in\mathcal{N}i}\beta_k^j\bar{\eta}_k^j\right)$$
$$\bar{\eta}_{k+1}^i = A\eta_k^i. \tag{33}$$

Similarly, since the innovation is nullified for nonobserving agents we have that $F_k^i = I_n \forall i \in \bar{\mathcal{O}}_k$ and so, the error dynamics for non observing agents are:

$$\begin{aligned}\eta_k^i &= \bar{\eta}_k^i + \frac{1}{\sum_{j\in\mathcal{N}_i}\beta_k^j}\sum_{j\in\mathcal{N}_i}\beta_k^j\left(\bar{F}_k\bar{\eta}_k^j - \bar{\eta}_k^i\right)\\ &= \bar{\eta}_k^i + \left(\frac{1}{\sum_{j\in\mathcal{N}_i}\beta_k^j}\bar{F}_k\sum_{j\in\mathcal{N}_i}\beta_k^j\bar{\eta}_k^j\right) - \bar{\eta}_k^i\\ &= \frac{1}{\sum_{j\in\mathcal{N}_i}\beta_k^j}\bar{F}_k\sum_{j\in\mathcal{N}i}\beta_k^j\bar{\eta}_k^j\\ \bar{\eta}_{k+1}^i &= A\eta_k^i,\end{aligned} \tag{34}$$

The joint error dynamics can now be constructed as such:

$$\begin{aligned}\eta_k &= \text{diag}\{F_k^iA\}_{i=1}^N\left(I_{Nn} - \left(\mathcal{D}_k^{-1}L_k^*\otimes I_n\right)\right)\eta_{k-1}\\ &= (I_N\otimes\bar{F}_kA)((I_N - \left(\mathcal{D}_k^{-1}L_k^*\right))\otimes I_n)\,\eta_{k-1}\\ &= \left((I_N - (\mathcal{D}_k^{-1}L_k^*))\otimes\bar{F}_kA\right)\eta_{k-1}.\end{aligned}$$

where $\mathcal{D}_k = \text{diag}\{d_k^i\}_{i=1}^N$ and

$$d_k^i = \begin{cases}1+\sum_{j\in\mathcal{N}_i}\beta_k^j & i\in\mathcal{O}_k\\ \sum_{j\in\mathcal{N}_i}\beta_k^j & i\in\bar{\mathcal{O}}_k\end{cases}.$$

By Assumption 1 we have that $d_k^i > 0$ for all agents, therefore the matrix $\mathcal{D}_k$ in invertible. Due to the properties of the Kronecker product, we have that $(I_N\otimes\bar{F}_kA)$ and $((I_N - (\mathcal{D}_k^{-1}L_k^*))\otimes I_n)$ commute. This leads to the following inequality,

$$\lim_{k\to\infty}\left\|\prod_k\left((I_N - (\mathcal{D}_k^{-1}L_k^*))\otimes\bar{F}_kA\right)\right\| \le \lim_{k\to\infty}\left\|\prod_k(\bar{F}_kA)\right\|\lim_{k\to\infty}\left\|\prod_k(I_N - (\mathcal{D}_k^{-1}L_k^*))\right\|.$$

The stability of the observers' NCLKF is ensured as $\lim_{k\to\infty}\left(\prod_k\bar{F}_kA\right) = 0$. Additionally, ETM (20) dictates the values of the instantaneous Laplacian L_k^*, however the row stochastic property of the matrix $\left(I_N - \mathcal{D}_k^{-1}L_k^*\right)$ is not affected. Thus, its spectral radius is always unity such that,

$$\rho\left(\lim_{k\to\infty}\left(\prod_k(I_N - \mathcal{D}_k^{-1}L_k^*\right)\right) = 1,$$

since the product of row-stochastic matrices is row-stochastic. Therefore,

$$\lim_{k\to\infty}\eta_k = \lim_{k\to\infty}\left(\prod_k\left(I_N - (\mathcal{D}_k^{-1}L_k^*)\right)\otimes\prod_k\bar{F}_kA\right)\eta_0 = 0.$$

and the error dynamics are asymptotically stable. ∎

We have shown that by using a decentralized consensus gain, we may approach unique scenarios in which some of the agents do not observe the process, and still obtain stability of the error dynamics. We strengthen our claim with a numerical example in the next section.

5 | SIMULATION RESULTS

Consider a group of 20 agents that observe a process with fourth-order dynamics such that,

$$x_{k+1} = \underbrace{\left(\begin{bmatrix} 0.9997 & 0.1000 \\ -0.0056 & 0.9997 \end{bmatrix} \otimes I_2\right)}_{A} x_k + \underbrace{\left(\begin{bmatrix} 0 \\ 1 \end{bmatrix} \otimes I_2\right)}_{B} w_k, \tag{35}$$

where the state vector x_k is composed of the position in $\mathbb{R}^2$ (first and second elements) and the velocity (third and fourth elements). The process initial state is set to be $x_0 = [0, 20, -4.71, 0]^T$. The initial covariance matrix for each agent is set to be $P_0^i = 2I_4$, and the agents' initial estimates are normally distributed about the initial state. Additionally, the process noise covariance is $Q = 0.01 \cdot I_2$. The sensors are randomly positioned in some field of interest (see Figure 4) where a communication link between two sensors exists only if their distance is below some threshold (<40 m). Furthermore, we consider two sensing models: (1) the homogeneous sensing model where each agent measure the process with the same observation model such that $R^i = R = 9$ and

$$H^i = H = \begin{bmatrix} 1 & 0 \end{bmatrix} \otimes I_2, \ i \in \{1, \dots, 20\},$$

and (2) a heterogeneous model where each agent with an even number measures the position while the agents with an odd number measure its velocity such that:

$$H^i = \begin{cases} \begin{bmatrix} 1 & 0 \end{bmatrix} \otimes I_2, & i \in \{1, 3, \dots, 19\} \\ \begin{bmatrix} 0 & 1 \end{bmatrix} \otimes I_2, & i \in \{2, 4, \dots, 20\} \end{cases}. \tag{36}$$

The measurement noise covariance for the ith agent is $R^i = \sqrt{i} I_2$.

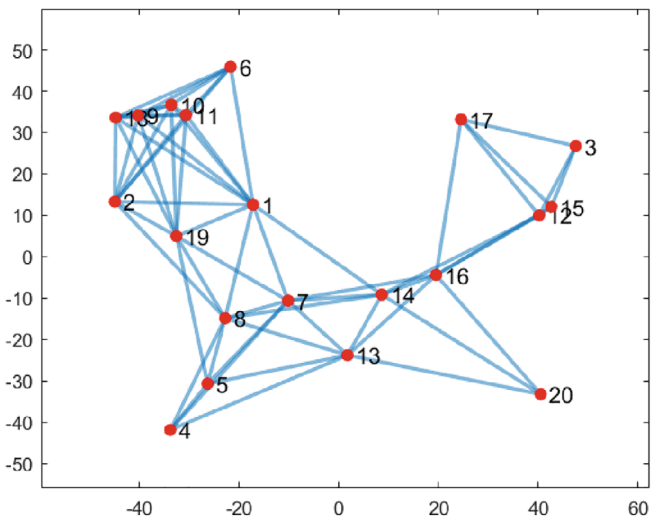

FIGURE 4 A sensor network of 20 agents randomly positioned.

We provide a comparison between six state estimators:

NCLKF: the noncooperative local Kalman filter with null consensus gain;
CKF the sub-optimal consensus Kalman filter consensus gain (7) with the factor (17).
ETCKF1: the sub-optimal event triggered consensus Kalman filter with consensus gain (7), consensus factor (17), and event-triggered condition (12);
ETCKF2: the sub-optimal event triggered consensus Kalman filter with consensus gain (18) and event-triggered condition (12);
ETDCKF: the sub-optimal event-triggered decentralized consensus Kalman filter with event triggered condition (21), $\delta = 0.2$, and the consensus gain (23);
POETCKF: the sub-optimal event triggered decentralized consensus Kalman filter with event triggered condition (30), $\delta = 0.2$, and the consensus gain (32).

The performance of these estimators was tested over 100 Monte-Carlo simulations in which the process and measurement noises were randomized. The compared performance measures are twofold. We compute the true averaged root mean squared error (Figure 5), calculated as

$$\texttt{RMSE} = \frac{1}{MC}\sum_{j=1}^{MC}\sqrt{\sum_{i=1}^{N}\mathbb{E}[(\eta^{i,j})^T\eta^{i,j}]},$$

where $\eta^{i,j}$ is the ith agent state estimation error for the jth run. Secondly, the agents local energy consumption expressed as total number of events per agent, denoted by $\#^i$ (Figure 6), calculated as

$$\#^i = \frac{1}{MC}\sum_{j=1}^{MC}\#^{i,j},$$

where MC is the number of Monte-Carlo runs and $\#^{i,j}$ is the ith agent's total number of triggered events for the jth run.

We begin our discussion with the homogeneous sensing model. Figure 5 illustrates the averaged RMSE for five estimators. As shown, the ETDCKF is preferable in performance over the ETCKF1 and ETCKF2 and even over the CKF. This is explained by the fact that for the ETDCKF, the consensus term is weighted according to the number of neighbors each agent has, while for the CKF all terms are weighted equally. Additionally, we see that the performance of the ETCKF1 is slightly better than that of ETCKF2. This result corresponds to the relatively low communication effort of this filter with respect to the others, as illustrated in Figure 6. Overall, in this sensing scheme all estimators show superiority over the NCLKF. The performance of all estimators is summarized in Table 1 where we compare the averaged communication effort computed in the following manner, $\frac{\sum_{i=1}^{N}\#^i}{400N}\cdot 100\%$, where 400 is the simulation time.

The process true and mean estimated trajectory (using homogeneous sensing model) is depicted in Figure 7, for a single run with both the ETCKF1 (Figure 7A) and the ETDCKF (Figure 7B). As shown, the filters provides reasonable tracking results.

Although we have proven the stability of ETDCKF for the case of homogeneous sensing model for all agents, we show in the following that in fact it provide reasonable results for the heterogeneous sensing model as well. Figure 8 illustrate the averaged RMSE for the discussed 5 estimators. As shown, the effect of the consensus, with respect to the NCLKF, is much more dominant here compared to the homogeneous case. This is understandable since the flow of information, in this scheme, provides new "insights" for some agents. Specifically, ETCKF2 shows degraded performance compared to ETCKF1, and slightly better performance than ETDCKF. This too corresponds to the relatively low communication effort of this filter with respect to the others. This is illustrated in Figure 9 where we see that estimators ETCKF1 and ETCKF2 are conservative while ETDCKF consumes a relative large amount of energy. What is interesting to see is that although the ETDCKF consumes more energy, its performance is degraded compared to ETCKF1, which indicates that the estimator structure has a dominant effect on performance for this scheme. The performance of all five estimators is summarized in Table 2.

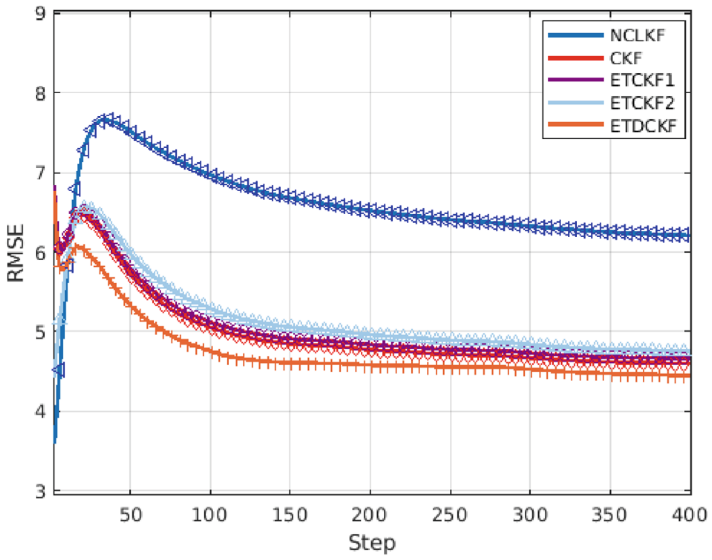

FIGURE 5 Root mean squared error, comparison between 5 state estimators over 100 Monte-Carlo runs with a homogeneous sensing model.

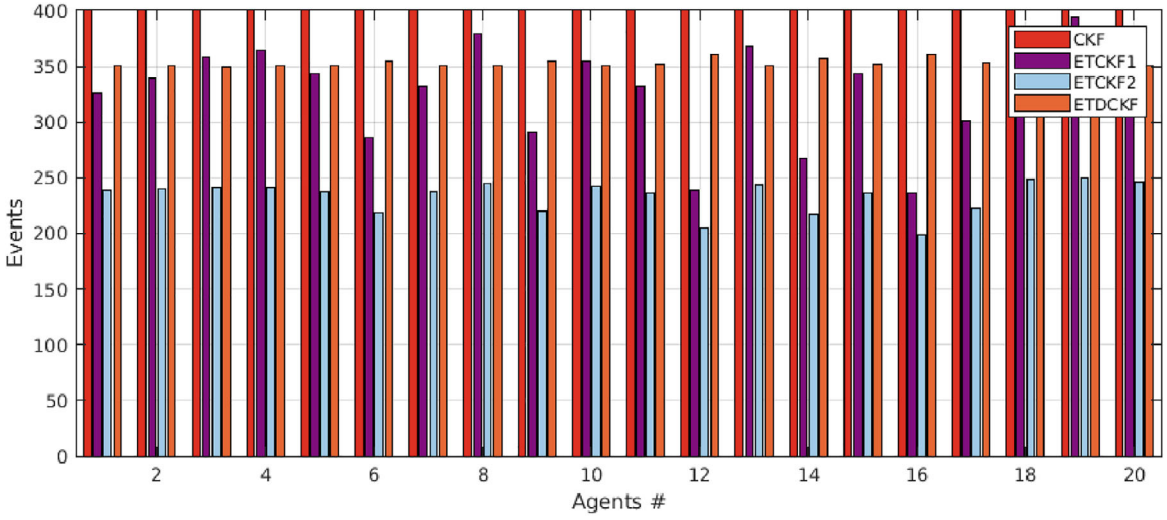

FIGURE 6 Total events per agent for a 400 step simulation—a comparison between 3 event triggered estimators and the CKF with a homogeneous sensing model.

TABLE 1 Estimators comparison for the homogeneous model.

Estimator	RMSE	Averaged com effort
NCLKF	6.2	0%
CKF	4.6	100%
ETCKF1	4.7	82%
ETCKF2	4.8	58%
ETDCKF	4.4	88%

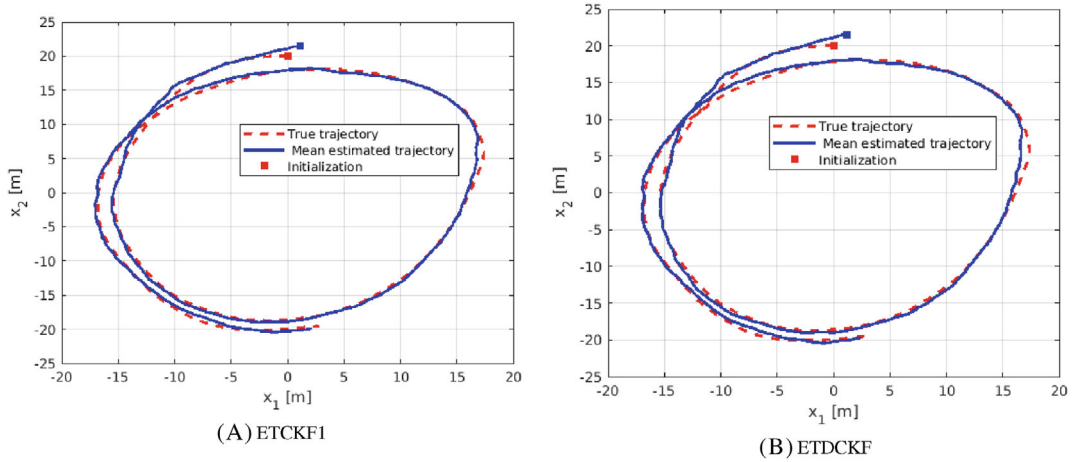

FIGURE 7 Trajectory of the true state and the agents' mean estimate utilizing ETCKF1 (A) and ETDCKF (B) for the homogeneous model.

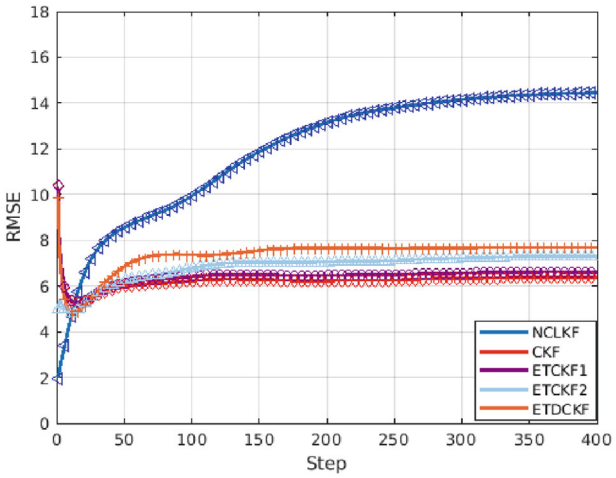

FIGURE 8 Root mean squared error, comparison between five state estimators over 100 Monte-Carlo runs with a heterogeneous sensing scheme.

The process true and mean estimated trajectory (using the heterogeneous sensing model) is depicted in Figure 10, for a single run with both the ETCKF1 (Figure 10A) and the ETDCKF (Figure 10B). As shown, the filter provides good tracking results.

To further demonstrate the robustness of the ETDCKF, we simulated an "unexpected" communication topology switch at two time instances, at $k = 50$ and $k = 150$; see Figure 11 for the different instances of the graph topology. We compared the sum of all agents MSE of a single run, with the heterogeneous sensing model, to that of the CKF and NCLKF, shown in Figure 12. In this scenario, the CKF estimator is maintaining the nominal communication topology of the Laplacian eigenvalues for calculating (17). After the first network switch, this leads the CKF to become unstable immediately afterwards, while the ETDCKF remains stable for the entire duration.

To conclude, we investigate the performance of the scenario where some of the agents do not obtain any measurements during the course of the process state evolution. To do so, we simulate a limitation where the agents cannot measure the process state once the physical distance between the process and the sensing agent is greater than some threshold. For the following analysis, we change the initial state vector to be $x_0 = [0, 40, -9.42, 0]^T$. We use the heterogeneous sensing model given in (36). The sensors are randomly positioned in some field of interest (see Figure 13) where a communication link between two sensors exists only if their distance is below 40 m. Additionally we have simulated an out of range value

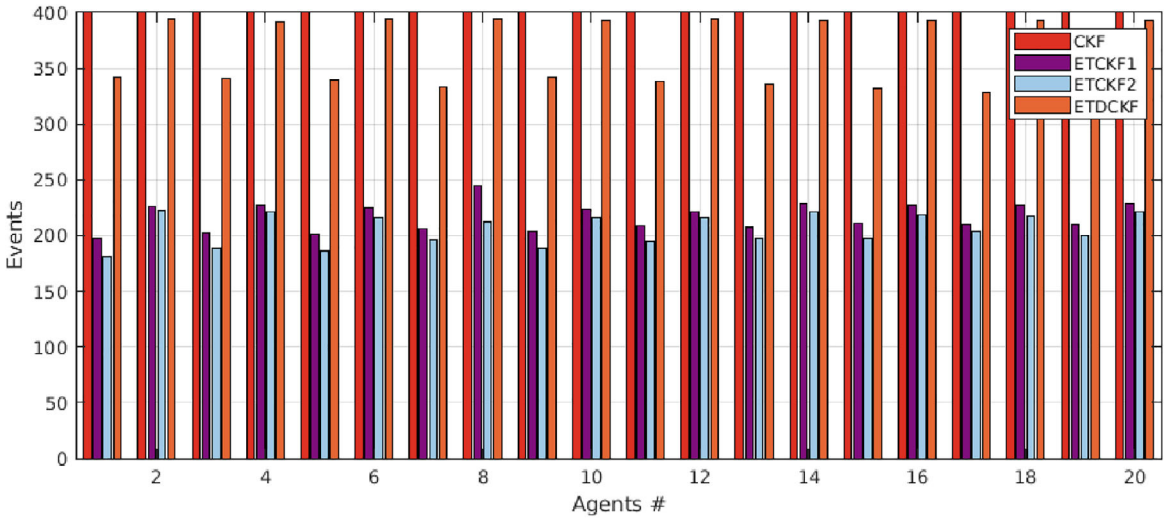

FIGURE 9 Total events per agent for a 400 step simulation–a comparison between three event triggered estimators and the CKF with a heterogeneous sensing scheme.

TABLE 2 Estimators comparison for the heterogeneous model.

Estimator	RMSE	Averaged com effort
NCLKF	14.4	0%
CKF	6.4	100%
ETCKF1	6.6	62%
ETCKF2	7.2	55%
ETDCKF	7.7	74%

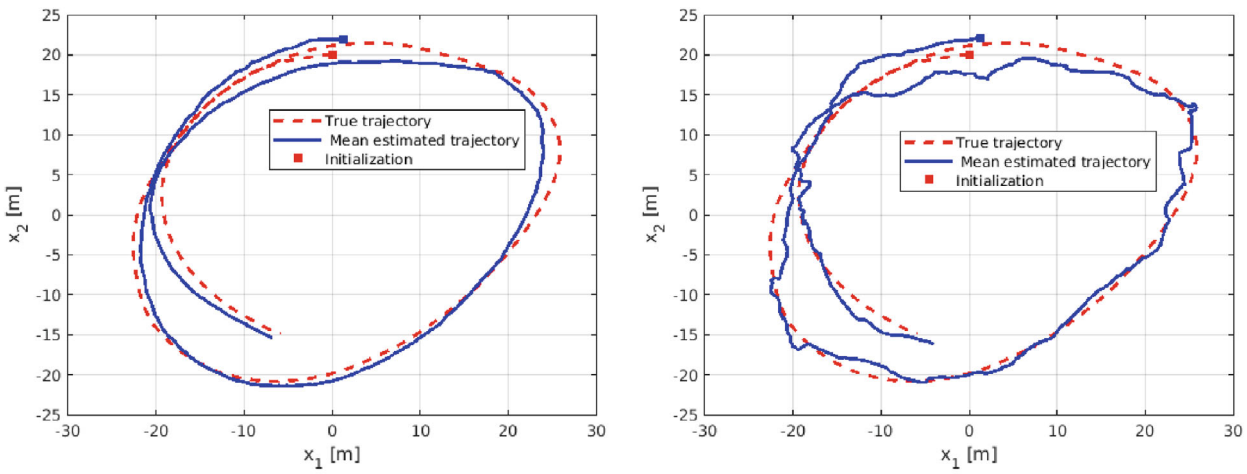

(A) ETCKF1 (B) ETDCKF

FIGURE 10 Trajectory of the true state and the agents' mean estimate utilizing ETCKF1 (A) and ETDCKF (B) for the heterogeneous model.

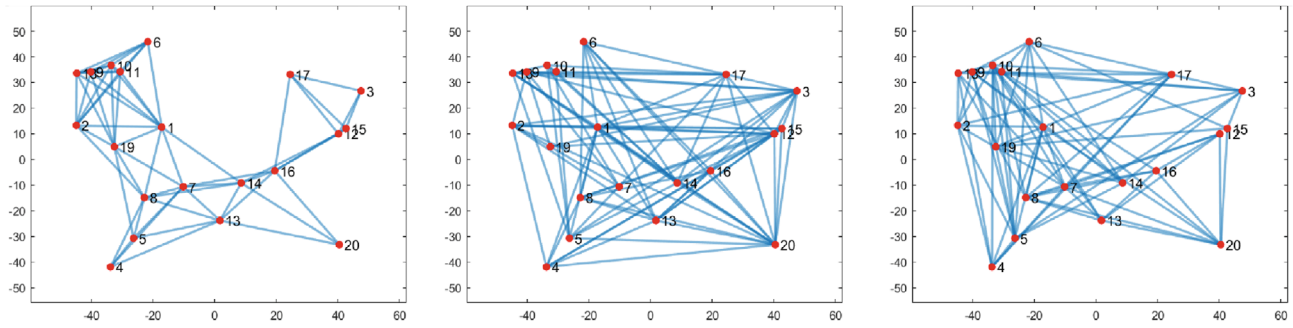

(A) Graph at $k = 1$. (B) Graph at $k = 50$. (C) Graph at $k = 150$.

FIGURE 11 Communication graph at time steps (A) 1–49, (B) 50–149, and (c) 150–400.

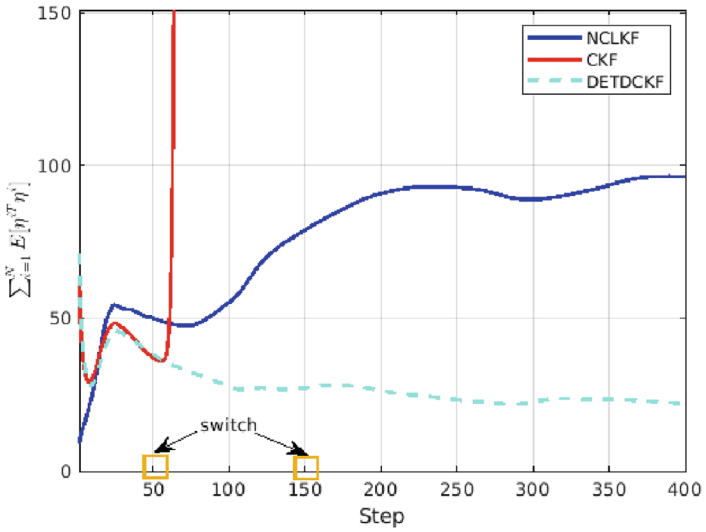

FIGURE 12 Sum of all agents mean squared error for 2 mid-run graph switch (at step 50 and at step 150), comparison between three state estimators for a single run.

of $r = 85$ m, such that, according to (27), measurements are available only when

$$\left\| \left(\begin{bmatrix} 1 & 0 \end{bmatrix} \otimes I_2 \right) x_k - p^i \right\| \leq 85. \tag{37}$$

This is illustrated for two time instances during the run in Figure 14 where nonobserving agents are marked in red.

Figure 15A depicts the events map of all agents as a function of time. Here, we find an averaged communication effort of 85%, which indicates that this scheme is effective compared to any time-triggered solution. Furthermore, Figure 15B compares the sum of all agents' MSE for two estimators: the NCLKF and POETCKF. As shown, the POETCKF provide reasonable results for a scenario with occasional partial nonobservability. This figure also captures the disadvantage in running the noncooperative estimator as the sum of MSE diverges since some of the agents' observability is lost.

To summarize this section, we have demonstrated superiority of our proposed centralized consensus gain compared to existing solutions and the noncooperative Kalman estimator for both homogeneous and heterogeneous sensing models. We have demonstrated robustness to time varying communication topology for the decentralized consensus gain. Finally, we have shown an effective and simple architecture for scenarios in which some agents are locally nonobservable.

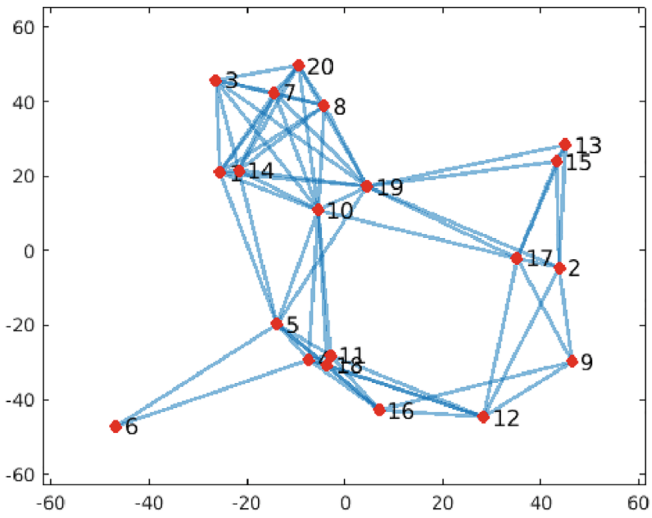

FIGURE 13 Available communication graph for a sensing network with 20 agents.

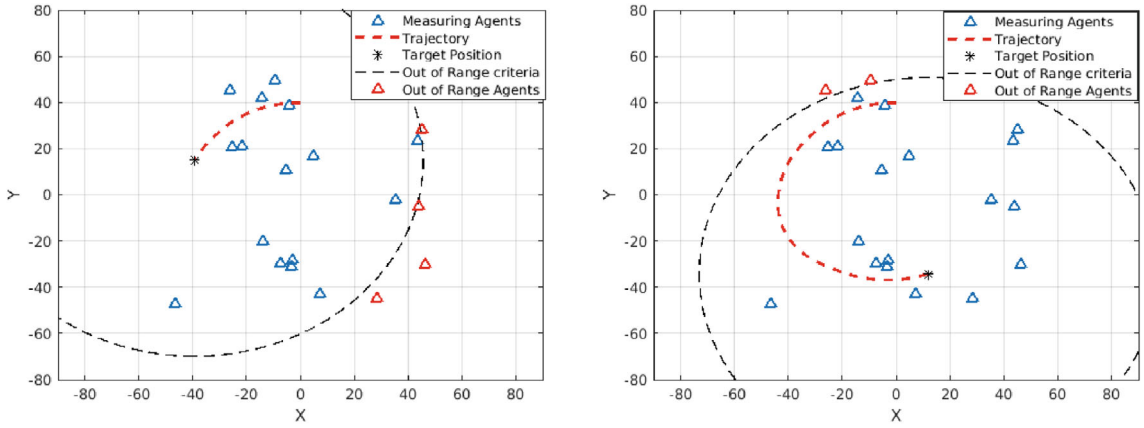

(A) $k = 50$. (B) $k = 150$.

FIGURE 14 Observing and nonobserving agents for an 85 m out of range limitation at $k = 50$ (A) and $k = 150$ (B).

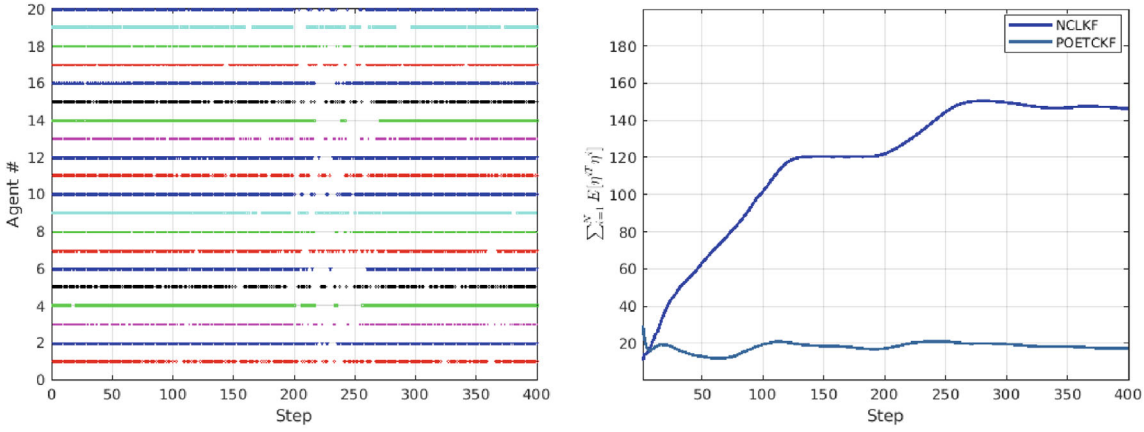

(A) POETCKF events per agent. (B) Sum of all agents MSE.

FIGURE 15 Results for the partial observability case according to an out of range criteria of 85 m. The results presented are the events distribution for all agents (left) and the sum of Mean Squared Error for all agents—comparison of the NCLKF and the POETCKF. (right).

6 | CONCLUSIONS

We have presented a widely common sub-optimal event-triggered consensus Kalman filter scheme and proposed new solutions for determining the consensus gain over a variety of data transfer architectures. In the centralized scheme, we provided a full stability analysis for a unified consensus gain along with suggesting an event triggering condition. In the decentralized scheme, we proposed a decentralized consensus gain which does not require global knowledge of graph properties. Additionally, we relaxed the assumption that all agents have full observability and constructed an event trigger architecture that deals with "blind" agents. Finally we have presented the effect of a low and high total event percentage with respect to performance by comparing our solution to both the noncooperative local Kalman filter and the continues consensus Kalman filter. For future research we recommend on expanding our results to include analysis for the heterogeneous sensing model case. Additionally our methods can be projected onto other distributed filters such as the consensus extended Kalman filter.

ACKNOWLEDGMENT

This work was supported by the Israel Science Foundation grant no. 2285/20.

CONFLICT OF INTEREST STATEMENT

There are no conflicts of interest.

DATA AVAILABILITY STATEMENT

The data that support the findings of this study are available from the corresponding author upon reasonable request.

ORCID

Aviv Priel https://orcid.org/0000-0002-5025-7563
Daniel Zelazo https://orcid.org/0000-0002-2931-245X

REFERENCES

1. Ousingsawat J, Campbell ME. On-line estimation and path planning for multiple vehicles in an uncertain environment. *Int J Robust Nonlinear Control*. 2004;14(8):741-766.
2. Jalalmaab M, Pirani M, Fidan B, Jeon S. Cooperative estimation of road condition based on dynamic consensus and vehicular communication. *IEEE Trans Intell Veh*. 2018;4(1):90-100.
3. Hao XC, Wu JZ, Chien CF, Gen M. The cooperative estimation of distribution algorithm: a novel approach for semiconductor final test scheduling problems. *J Intelligent Manufact*. 2014;25(5):867-879.
4. Chen H, Wang X, Li Z, Chen W, Cai Y. Distributed sensing and cooperative estimation/detection of ubiquitous power internet of things. *Protection Control Modern Power Syst*. 2019;4(1):1-8.
5. Yan J, Xu Z, Wan Y, Chen C, Luo X. Consensus estimation-based target localization in underwater acoustic sensor networks. *Int J Robust Nonlinear Control*. 2017;27(9):1607-1627.
6. Bahr A, Walter MR, Leonard JJ. Consistent cooperative localization. *2009 IEEE International Conference on Robotics and Automation*. IEEE; 2009:3415-3422.
7. Sun T, Chen LJ, Han CC, Gerla M. Reliable sensor networks for planet exploration. *Proceedings. 2005 IEEE Networking, Sensing and Control*. Vol 2005. IEEE; 2005:816-821.
8. Ribeiro A, Giannakis GB. Bandwidth-constrained distributed estimation for wireless sensor networks-part I: Gaussian case. *IEEE Trans Signal Process*. 2006;54(3):1131-1143.
9. Zhou HY, Luo DY, Gao Y, Zuo DC. Modeling of node energy consumption for wireless sensor networks. *Wireless Sensor Network*. 2011;3(1):18.
10. Lemmon M. Event-triggered feedback in control, estimation, and optimization. *Networked control systems*. Springer; 2010:293-358.
11. Molin A, Hirche S. An iterative algorithm for optimal event-triggered estimation. *IFAC Proc Vol*. 2012;45(9):64-69.
12. Weimer J, Araújo J, Johansson KH. Distributed event-triggered estimation in networked systems. *IFAC Proc Vol*. 2012;45(9):178-185.
13. Olfati-Saber R. Distributed Kalman filtering for sensor networks. *2007 46th IEEE Conference on Decision and Control*. IEEE; 2007:5492-5498.
14. Alighanbari M, How JP. Unbiased Kalman consensus algorithm. *J Aerospace Comput Informat Commun*. 2008;5(9):298-311.
15. Li W, Jia Y, Du J. Event-triggered Kalman consensus filter over sensor networks. *IET Control Theory Appl*. 2016;10(1):103-110.
16. Zhang C, Jia Y. Distributed Kalman consensus filter with event-triggered communication: formulation and stability analysis. *J Franklin Inst*. 2017;354(13):5486-5502.
17. Liang Y, Li Y, Chen S, Qi G, Sheng A. Event-triggered Kalman consensus filter for sensor networks with intermittent observations. *Int J Adapt Control Signal Process*. 2021;35(8):1478-1497.

18. Meng X, Chen T. Optimality and stability of event triggered consensus state estimation for wireless sensor networks. *2014 American Control Conference*. IEEE; 2014:3565-3570.
19. Deshmukh R, Kwon C, Hwang I. Optimal discrete-time Kalman consensus filter. *2017 American Control Conference (ACC)*. IEEE; 2017:5801-5806.
20. Hu J, Jia C, Liu H, Yi X, Liu Y. A survey on state estimation of complex dynamical networks. *Int J Syst Sci*. 2021;52(16):3351-3367.
21. Hu J, Wang Z, Liu GP, Jia C, Williams J. Event-triggered recursive state estimation for dynamical networks under randomly switching topologies and multiple missing measurements. *Automatica*. 2020;115:108908.
22. Zhang H, Hu J, Liu H, Yu X, Liu F. Recursive state estimation for time-varying complex networks subject to missing measurements and stochastic inner coupling under random access protocol. *Neurocomputing*. 2019;346:48-57.
23. Beineke LW, Wilson RJ, Cameron PJ, et al. *Topics in algebraic graph theory. 102*. Cambridge University Press; 2004.
24. Olfati-Saber R, Fax JA, Murray RM. Consensus and cooperation in networked multi-agent systems. *Proc IEEE*. 2007;95(1):215-233.
25. Olfati-Saber R. Kalman-consensus filter: Optimality, stability, and performance. *Proceedings of the 48h IEEE Conference on Decision and Control (CDC) held jointly with 2009 28th Chinese Control Conference*. IEEE; 2009:7036-7042.
26. Priel A, Zelazo D. An Improved Distributed Consensus Kalman Filter Design Approach. *2021 60th IEEE conference on Decision and Control*. IEEE; 2021:502-507.
27. Wenshuang L, Shanying Z, Cailian C, Xinping G. Distributed consensus filtering based on event-driven transmission for wireless sensor networks. *Proceedings of the 31st Chinese Control Conference*. IEEE; 2012:6588-6593.
28. Siddik SM. *Kullback-Leibler Information Function and the Sequential Selection of Experiments to Discriminate Among Several Linear Models*. PhD Thesis. University of Pennsylvania, USA; 1972.
29. Willner D, Chang C, Dunn K. Kalman filter algorithms for a multi-sensor system. *1976 IEEE Conference on Decision and Control Including the 15th Symposium on Adaptive Processes*. IEEE; 1976:570-574.

How to cite this article: Priel A, Zelazo D. Event-triggered consensus Kalman filtering for time-varying networks and intermittent observations. *Int J Robust Nonlinear Control*. 2023;33(13):7430-7451. doi: 10.1002/rnc.6762